ChemPubSoc Europe

DOI: 10.1002/cbic.201700677

CHEMBIOCHEM Full Papers

Deletion of the C26 Methyl Substituent from the Bryostatin Analogue Merle 23 Has Negligible Impact on Its Biological Profile and Potency

Xiguang Zhao[+],[b] Noemi Kedei[+],[a] Alexandra Michalowski,[a] Nancy E. Lewin,[a] Gary E. Keck,[b] and Peter M. Blumberg*[a]

Important strides are being made in understanding the effects of structural features of bryostatin 1, a candidate therapeutic agent for cancer and dementia, in conferring its potency toward protein kinase C and the unique spectrum of biological responses that it induces. A critical pharmacophoric element in bryostatin 1 is the secondary hydroxy group at the C26 position, with a corresponding primary hydroxy group playing an analogous role in binding of phorbol esters to protein kinase C. Herein, we describe the synthesis of a bryostatin homologue in which the C26 hydroxy group is primary, as it is in the phorbol esters, and show that its biological activity is almost indistinguishable from that of the corresponding compound with a secondary hydroxy group.

Introduction

The bryostatins are a family of complex macrolactone marine natural products originally isolated through the pioneering efforts of Pettit and co-workers.[1] The flagship member of the family, bryostatin 1 (**1**), has received enormous attention due to the range of important and medicinally relevant biological activities it induces. Originally isolated due to the potent anticancer activity shown by extracts of the marine organism *Bugula neritina* against a cancer cell line, it has since been found to be a potent activator of protein kinase C (PKC) and other proteins that, like PKC, are activated by diacylglycerols (DAGs).[2,3] As a potent activator of PKC, the biological activities of bryostatin 1 share similarities with those of other known high affinity ligands for PKC (such as phorbol esters, exemplified by phorbol 12-myristate 13-acetate (PMA; **2**)), but importantly, unlike the phorbol esters, bryostatin 1 is not tumor-promoting in a two-stage mouse model for carcinogenesis.[4] Bryostatin 1 has been utilized in numerous clinical trials for cancer[3] and has more recently been of interest with respect to Alzheimer's disease[5] and HIV infection.[6] Other members of the bryostatin family mainly differ from bryostatin 1 in having different substituents at C7 and/or C20, although some, such as bryostatin 3, are more heavily modified. However, all possess the same basic macrocyclic lactone core structure, incorporating three pyran rings. Pettit named this common core structural feature a "bryopyran" motif (Scheme 1).

As might be expected, the complex structure and potent biological activity of bryostatin 1 has led to great interest in the chemical synthesis of these compounds.[7] The first synthesis of a bryostatin, bryostatin 7, was reported by Masamune and co-workers in 1990.[8] Despite the intense interest in these compounds, it was not until 1998 that a second synthesis was reported, this of bryostatin 2, by Evans and co-workers.[9] This was followed in 2000 by a synthesis of bryostatin 3 by Yamamura and co-workers.[10] It was roughly a decade later before other syntheses of bryostatins were reported. The first total synthesis of bryostatin 1 was reported by Keck and co-workers in 2011.[11] Other elegant total syntheses in this area were also published, including bryostatin 16 by Trost,[12] bryostatin 7 by Krische,[13] bryostatin 9 by Wender,[14] and bryostatin 8 by Song.[15]

However, in 1998, Wender and co-workers reported the synthesis of a simplified analogue of bryostatin 1 (**7**) in which the B-ring pyran was replaced by a 1,3-dioxane for ease of synthesis of this acetal subunit.[16] This bryostatin analogue was shown to have similar affinity for PKCs (by using a mixture of isozymes isolated from rat brain) to that of bryostatin 1 (3 vs. 1.4 nM). Subsequently, numerous such acetal analogues of bryostatin 1 were prepared by the Wender group, most notably, perhaps, acetal **8**, which was dubbed "pico" by Wender et al. to reflect the reported very high PKC binding affinity of 0.25 nM (250 pM).[17] The less potent original acetal analogue, **7**, was then named "nano"; these identifiers were subsequently used in numerous Wender publications and remain in use today (Scheme 2).

Our own interest in these fascinating compounds originally focused on the development of methodology that might be of

[a] Dr. N. Kedei,[+] Dr. A. Michalowski, N. E. Lewin, Dr. P. M. Blumberg
Laboratory of Cancer Biology and Genetics
Center for Cancer Research, National Cancer Institute
Building 37, Room 4048, 37 Convent Drive MSC4255
Bethesda, MD 20892-4255 (USA)
E-mail: blumberp@dc37a.nci.nih

[b] Dr. X. Zhao,[+] Dr. G. E. Keck
Department of Chemistry, University of Utah
315 South 1400 East, RM 2020, Salt Lake City, Utah 84112 (USA)

[+] These authors contributed equally to this work.

Supporting information and the ORCID identification numbers for the authors of this article can be found under https://doi.org/10.1002/cbic.201700677.

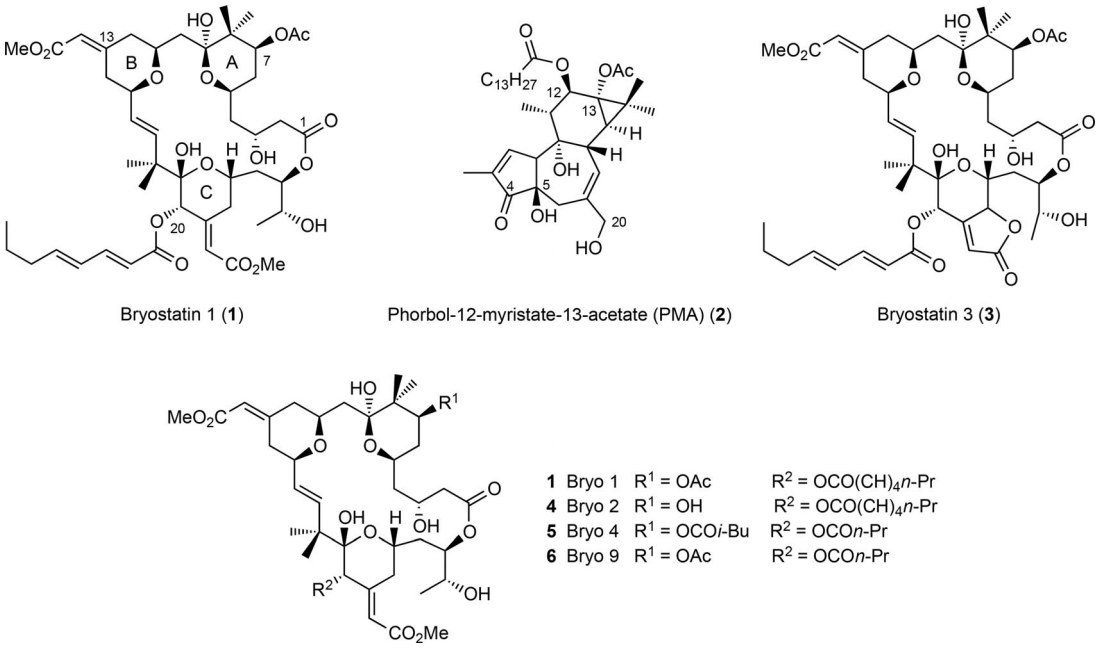

Scheme 1. Structures of representative bryostatins and PMA.

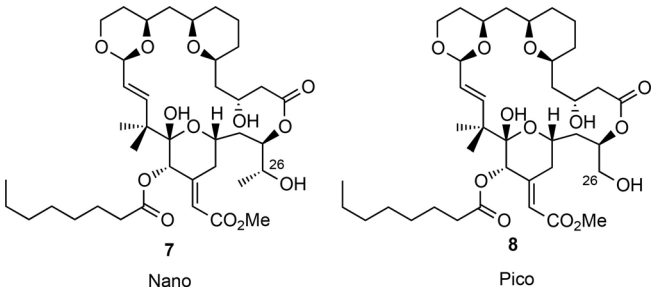

Scheme 2. Structures of the Wender acetal analogues nano (**7**) and pico (**8**).

general utility in accessing the bryopyran core structures. The most powerful of these methodologies, termed "pyran annulation", described a highly convergent asymmetric methodology by which a hydroxyallyl silane (**11**) could be annealed with an aldehyde (**12**) under acidic conditions to provide a disubstituted pyran (**13**) of the type that occurs repeatedly in the bryopyran core structure. One method by which the hydroxyallyl silanes (**11**) were readily available was by nucleophilic addition of a conjunctive reagent (**10**) to an aldehyde (**9**); thus, overall, two aldehydes plus the conjunctive reagent were annealed to provide a pyran (Scheme 3). This initial report[18] was followed by a demonstration of application to the synthesis of the bryopyran core structure of the bryostatins[19] and then to the first

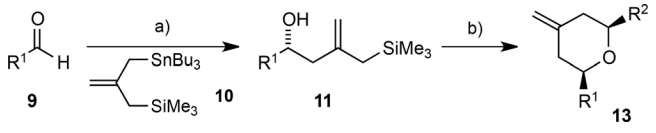

Scheme 3. Pyran annulation. a) BITIP, CH_2Cl_2; b) R_2CHO (**12**), TMSOTf, Et_2O, −78 °C.

biologically active bryostatin analogues that possessed the core bryopyran carbon skeleton.[20] The lead analogue here, Merle 23, also possessed the unusual dienoate C20 substituent found in bryostatin 1 but lacked much of the functionalization in the A and B rings. This compound was found to have binding affinity for the PKCα isozyme, very similar to that of bryostatin 1 (0.70 vs. 0.4 nM), but surprisingly functioned like the tumor-promoting ligand PMA in U937 lymphoma cells, rather than like bryostatin 1. U937 cells are known[21] to provide a well-characterized biological system that discriminates between PMA and bryostatin 1 activities: PMA induced attachment and blocked proliferation of these cells, whereas bryostatin 1 had little effect in either the attachment or the proliferation assay. Moreover, bryostatin 1 blocked the effect of PMA when the U937 cells were treated with the two agents together, thus confirming that bryostatin 1 was not simply being degraded. At the same time, Wender also reported the synthesis of some bryopyrans by using our pyran annulation strategy, but in an intramolecular context, and described their binding affinity for a mixture of PKC isozymes from rat brain.[22] Subsequent studies from our group, which examined substituent effects on biological activity, led to a model in which the lower portion of the bryopyran was largely responsible for its binding to PKC, whereas the functional response in living cells depended heavily upon substitution in the upper half of the structure.[23]

The 2008 paper from the Wender group also made an important correction, namely, that there really was no "pico". A table footnote directs the reader to another table footnote in the Supplementary Material that indicates that the original report of binding affinity for "pico" was believed to be an error, and that the new binding affinity was 3.1 nM, that is, essentially the same as that for "nano". However, a report from the Wender lab published subsequent to this paper still re-

ferred to the 0.25 nM value originally claimed for pico.[24] This confusing state of affairs, and the lack of other biological characterization for pico, prompted us to examine the same structural change on the bryopyran platform, particularly as Merle 23 had been extensively characterized in terms of the biological effects it induced.[25] Here, we report the synthesis and biological activity of the new bryopyran analogue, Merle 41, in which the C26 methyl substituent was deleted from structure Merle 23 (Scheme 4).

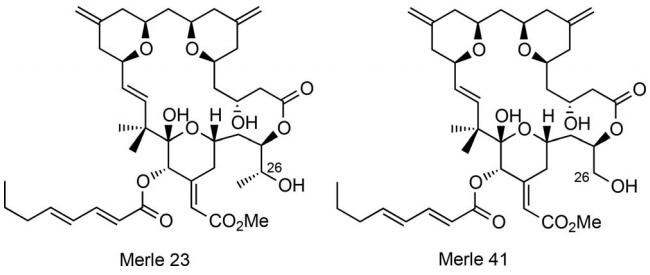

Scheme 4. Structures of Merle 23 and Merle 41.

Results

Synthesis of bryopyran Merle 41

The synthetic plan for Merle 41 followed the scheme demonstrated in 2005, utilizing two consecutive pyran annulations to prepare the B and C rings. However, the absence of the C26 stereogenic center required that the very beginning steps of the synthesis (which occur in our C ring fragment) be reworked. Previously, we had used a commercially available starting material containing the C26 stereogenic center, and this stereochemistry was then utilized to construct additional stereogenic centers through a series of diastereoselective reactions. With this center absent, an asymmetric approach to generating the C25 stereogenic center was required (Scheme 5).

The synthesis of the C ring segment commenced from allyl alcohol (**17**; Scheme 6). The hydroxy group was protected, after which ozonolysis afforded aldehyde **18**. The requisite

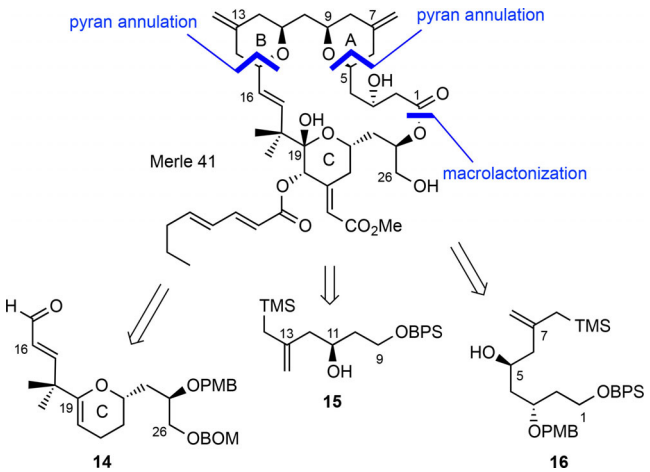

Scheme 5. Retrosynthetic plan for synthesis of Merle 41.

stereocenter at C25 was then established by using a catalytic asymmetric allylation (CAA) reaction,[26] which afforded the desired homoallylic alcohol (**19**) in excellent yield (93%) and essentially as a single enantiomer (99% *ee*). The new hydroxy group was protected as a PMB ether, with an eye toward conducting a diastereoselective nucleophilic addition to aldehyde **20**, available from the olefin by oxidative cleavage. Unfortunately, neither chelation-controlled nor non-chelation-controlled reaction conditions provided a satisfying level of stereoselectivity upon addition to aldehyde **20**. Finally, a second CAA reaction was applied to afford alcohol **21** as essentially a single diastereomer (minor isomer not detected).

After conversion of the free hydroxy group to a TBS ether, the alkene was regioselectively hydroformylated to give aldehyde **22** in 87% yield.[27] Next, we carried out a prenylation reaction to add a reverse prenyl group to aldehyde **22**. Although we had done such reactions previously using indium metal and an allylic halide, here we found that the use of inexpensive zinc dust in an aqueous medium gave excellent results; subsequent Swern oxidation of the resulting secondary alcohol afforded ketone **23**. Ozonolysis of the vinyl group, followed by a phosphonate Wittig reaction on the resulting aldehyde, afforded α,β-unsaturated thiol ester **24** in 86% yield over the two steps.[28] After removal of the TBS group by reaction with aqueous HF buffered with pyridine, acid-promoted cyclization of the hydroxy ketone with concomitant dehydration was accomplished by using CSA in toluene at reflux to afford glycal **25**. Low temperature reduction with DIBAL in dichloromethane then gave the desired enal (**14**; Scheme 6).

The hydroxyallylstannane required for the pyran annulation had been previously prepared by CAA reaction in our labs.[18,19] However, several examples of pyran annulation reactions, conducted with glycals such as **14** as substrates, had been examined previously and had generally proven to be problematic, in that yields were significantly lower than for most other cases examined. Similar complications were observed in attempted pyran annulations with **14**. Thinking that the problem could potentially be decomposition due to the presence of acid-sensitive regions of the substrate, we examined the use of various additives in the pyran annulation by using substrate **14**. It was found that the use of substoichiometric amounts of pyridine greatly improved the yields and reproducibility of this reaction, with the yield improvement being in the 20–30% range. Under optimal conditions, the desired pyran product **26** was obtained much more cleanly, and in 93% isolated yield (Scheme 7).

To avoid the impediment of the labile glycal in the remaining synthetic steps, the C ring was fully functionalized at this point. After chemoselective epoxidation and methanolysis in situ, the resulting ketal was subjected to a catalytic amount of PPTS to enrich the mixture of diastereomers (at C19) in favor of the desired and thermodynamically more stable isomer. Dess–Martin periodinane (DMP) oxidation then provided ketone **27**.[29] This sequence of three steps was accomplished in excellent (89%) yield. To complete the elaboration of the C ring, an aldol reaction with freshly distilled methyl glyoxalate was used to give enoate **28** in 76% isolated yield. Luche

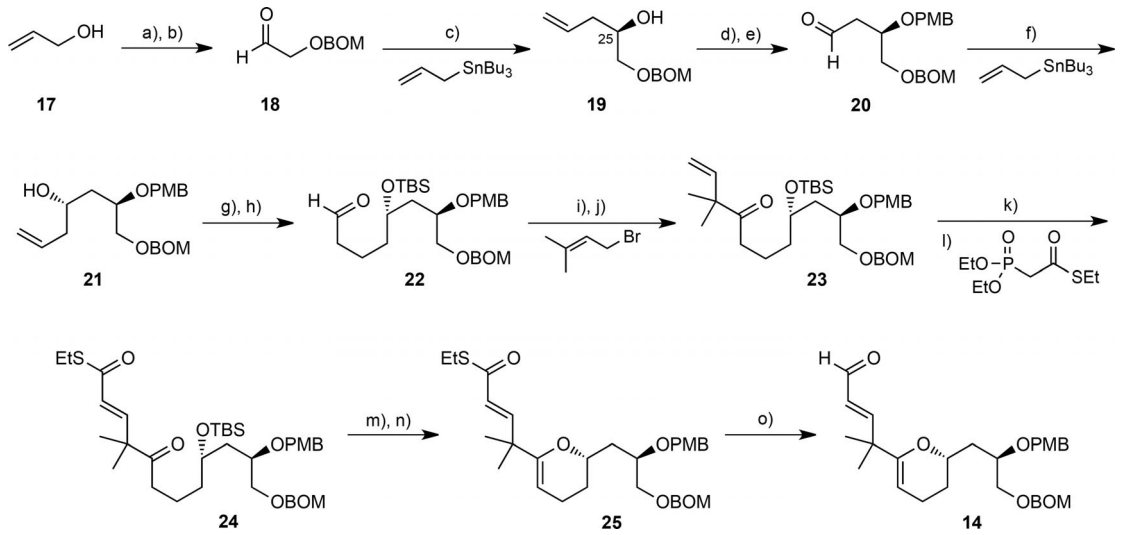

Scheme 6. Synthesis of the C ring fragment. a) NaH, BOMCl, THF, 0 °C–RT; b) O_3, CH_2Cl_2, −78 °C, then DMS (84% over 2 steps); c) (*R*)-BITIP, TFA, 4 Å MS, CH_2Cl_2, −78 °C to −30 °C (93%, 99% *ee*); d) KH, PMBBr, THF, 0 °C (96%); e) O_3, CH_2Cl_2, −78 °C, then PPh_3 (83%); f) (*S*)-BITIP, TFA, 4 Å MS, CH_2Cl_2, −78 to −30 °C (89%, >99% *dr*); g) TBSCl, Im, DMF, RT (99%); h) BIPHEPHOS, CO/H_2 (1:1), $Rh(CO)_2(acac)$, THF, 60 °C (87%); i) Zn, NH_4Cl (aq.), THF, RT; j) $(COCl)_2$, DMSO, NEt_3, CH_2Cl_2, −78 °C (91% over 2 steps); k) O_3, PPh_3, CH_2Cl_2, −78 °C; l) NaH, THF, 0 °C (86% over 2 steps); m) HF (aq.), Py, MeCN, RT; n) CSA, PhMe, reflux (79% over 2 steps); o) DIBAL, CH_2Cl_2, −78 °C (80%).

reduction of the ketone[30] gave an unstable alcohol, which was immediately esterified with the requisite octadienoic acid under Yamaguchi conditions.[31] The desired C20 ester **29** was obtained in an excellent 93% yield over this two-step sequence.

The stage was now set for incorporation of the A ring. Removal of the BPS group by using ammonium fluoride in methanol at reflux gave the corresponding alcohol (92% yield), which was oxidized by using Dess–Martin reagent to the corresponding aldehyde. At this point, it was necessary to perform a protecting group swap of the PMB group in aldehyde **30**, due to the presence of another PMB group on the hydroxyallyl silane partner for the pyran annulation. This was accomplished by removal of the PMB group by reaction with DDQ, followed by silylation of the alcohol with TBS triflate at −78 °C, to give aldehyde **31**.

An A ring hydroxyallyl silane was easily prepared from homoallylic alcohol **34**, itself available through a CAA reaction as shown (Scheme 8). The alcohol was protected as a PMB ether to allow for a high level of diastereoselectivity in the subsequent allylation of aldehyde **35** (Scheme 8).

Thus, after introduction of the PMB group, the vinyl group was cleaved by ozonolysis to afford aldehyde **35**. Chelation-controlled addition of silyl stannane reagent **10**, promoted by magnesium bromide etherate in dichloromethane at −78 °C, afforded essentially exclusively (>99:1) the desired diastereomer of hydroxyallyl silane **36**, as a consequence of chelation control in addition to a preformed magnesium chelate.[32]

With both aldehyde **31** and β-hydroxyallylsilane **36** in hand, the second pyran annulation was conducted to afford tris pyran **37** in excellent yield (90%) under the modified (pyridine additive) conditions (Scheme 9). The BPS silyl ether at C1 was selectively deprotected by NH_4F, and the resulting alcohol was subject to DMP oxidation to afford aldehyde **38** in 57% yield over two steps. The aldehyde was then oxidized to the corresponding carboxylic acid under Pinnick conditions.[33] Next, the removal of the C25 TBS group furnished a seco-acid, which then underwent macrolactonization according to Yamaguchi's protocol under high dilution techniques (slow addition by syringe pump). These three steps transpired in amazingly high overall yield, affording the macrolactone **39** in 95% isolated yield. With the bryopyran skeleton now complete, all that remained was removal of the final three protecting groups. This was accomplished by initial DDQ-mediated PMB removal, followed by a global deprotection with $LiBF_4$,[34] to afford the des-methyl analogue Merle 41 in 69% yield.

Biological characterization of Merle 41

Merle 41 bound to PKCα with a K_i value of (0.73 ± 0.05) nM ($n = 3$ experiments). This value closely matches the K_i of (0.70 ± 0.06) nM that we reported previously for Merle 23.[20] We previously described that bryostatin 1 and bryostatin 7 showed little PKC isoform selectivity,[23b] with no more than a threefold difference in K_i values for human PKCβII, PKCδ, and PKCε compared to that for human PKCα. In preliminary experiments, we found that this was likewise the case for Merle 41. K_i values of Merle 41 for human PKCβII, PKCδ, and PKCε assayed in vitro were (2.1 ± 0.6), (0.8 ± 0.2), and (0.9 ± 0.2) nM, respectively. Although these measurements were not carried out in parallel with the above, and thus do not provide a precise comparison, they give no indication of substantial in vitro binding selectivity among PKC isoforms for Merle 41.

The Toledo cell line is derived from a non-Hodgkin's B cell lymphoma. It is among the most sensitive cell lines for growth inhibition by phorbol ester and, unlike leukemia cell lines such as U937, K562, or MV-4–11,[35] is similarly growth inhibited by bryostatin 1.[36,37] Merle 41 and Merle 23, like PMA and bryosta-

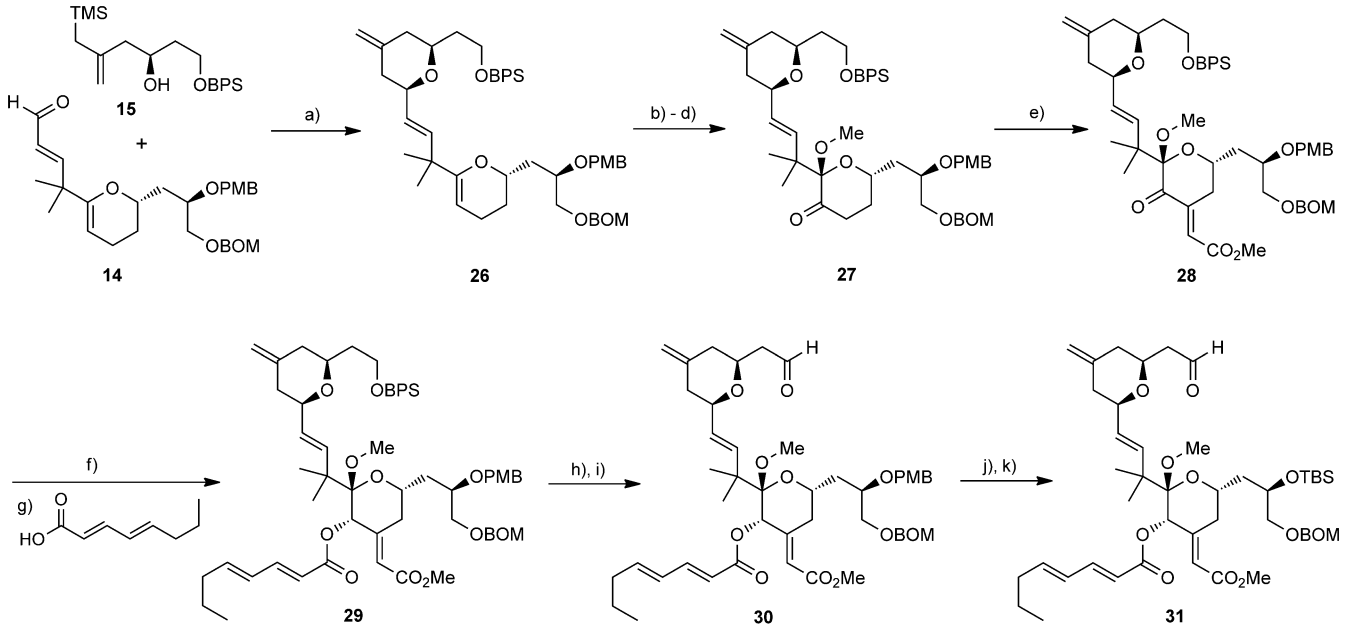

Scheme 7. Pyran annulation and C ring elaboration. a) TMSOTf, Py, Et_2O, −78 °C (93%); b) *m*-CPBA, MeOH, CH_2Cl_2, −10 °C; c) PPTS, MeOH, RT; d) DMP, *t*BuOH, Py, CH_2Cl_2, RT (89% over 3 steps); e) MeO_2CCHO, K_2CO_3, MeOH, THF, RT (76%, *E*/*Z* > 95:5); f) $NaBH_4$, $CeCl_3 \cdot 7H_2O$, MeOH, −78 °C; g) 2,4,6-$(Cl_3C_6H_2)COCl$, DMAP, NEt_3, PhMe, RT (93% over 2 steps); h) NH_4F, MeOH, reflux (92%); i) DMP, *t*BuOH, Py, CH_2Cl_2, RT (97%); j) DDQ, pH 6 buffer, CH_2Cl_2, 0 °C (98%); k) TBSOTf, 2,6-lutidine, CH_2Cl_2, −78 °C (90%).

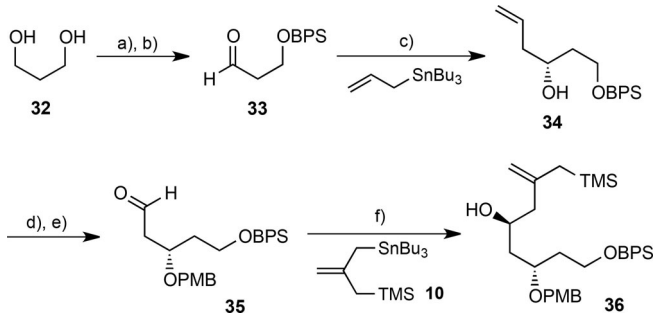

Scheme 8. Preparation of A ring allyl silane. a) NaH, BPSCl, THF, RT (96%); b) $(COCl)_2$, DMSO, NEt_3, CH_2Cl_2, −78 °C (97%); c) TFA, (*R*)-BITIP, 4 Å MS, CH_2Cl_2, −30 °C (98%, 98% *ee*); d) PMB-imidate, PhMe, $Sc(OTf)_3$, 0 °C (76%); e) O_3, DMS, CH_2Cl_2, −78 °C (92%); f) CH_2Cl_2, $MgBr_2 \cdot OEt_2$, −78 °C (85%, > 99% *dr*).

tin 1, inhibited Toledo cell growth (Figure 1 A). Merle 41 closely resembled Merle 23, both in potency and in the extent of growth inhibition. Unlike the Toledo cells, U937 promyelocytic leukemia cells respond to phorbol ester with growth inhibition and cell attachment, whereas bryostatin 1 causes little growth inhibition and almost no cell attachment. Merle 41 elicited a response virtually identical to that to Merle 23 (Figure 1 B and C). For both compounds, U937 cell growth was inhibited almost to the level caused by PMA but with a somewhat biphasic dose response, with reduced inhibition at 100 or 1000 nM. Attachment was induced to the same level as for PMA, but again, the dose–response was biphasic, with reduced attachment at 300 nM or above. The combination of PMA plus Merle 41 or Merle 23 gave a response similar to that of Merle 23 or Merle 41 alone, and the pattern of partial antagonism of the PMA response at high concentrations of Merle 23 or Merle 41 was the same for each.

TNFα was released onto the medium of the U937 cells in response to PMA and contributed to growth inhibition. Merle 41 and Merle 23 displayed identical dose–response curves for release of TNFα, with absolute maximal levels of release of (65.2 ± 2.6)% and (66.6 ± 2.6)%, respectively, of that for PMA (Figure 1 D). Once again, in combination with PMA, both compounds reduced the level of TNFα release in response to PMA to the level induced by the compound alone. By all of these measures, Merle 41 was very similar to Merle 23.

PMA, bryostatin 1, and Merle 23 caused distinct patterns of downregulation of PKC isozymes in the human prostate cancer cell line LNCaP as a function of time.[25] As previously observed, PKCδ was downregulated by PMA, bryostatin 1 caused biphasic downregulation of PKCδ with protection at higher bryostatin 1 doses, and Merle 23 caused more extensive downregulation of PKCδ than did either PMA or bryostatin 1 (Figure 2 A). Merle 41 acted similarly to Merle 23. PKCα was downregulated by PMA, bryostatin 1 was more potent at PKCα downregulation, and Merle 23 was less potent than either and indeed, at low doses, caused a modest increase in PKCα (Figure 2 B). Merle 41 again acted similarly to Merle 23. PKCε showed modest downregulation in response to PMA, bryostatin 1 caused even less downregulation, and Merle 23 resembled PMA in inducing weak PKCε downregulation (Figure 2 C). Merle 41 showed a pattern of response identical to that of Merle 23. Finally, PMA caused strong downregulation of PKD1. Bryostatin 1 and Merle 23 caused little PKD1 downregulation (Figure 2 D). Merle 41, again, closely paralleled Merle 23.

Although the data clearly showed that Merle 41 resembled Merle 23 in its downregulation of the PKC isoforms examined,

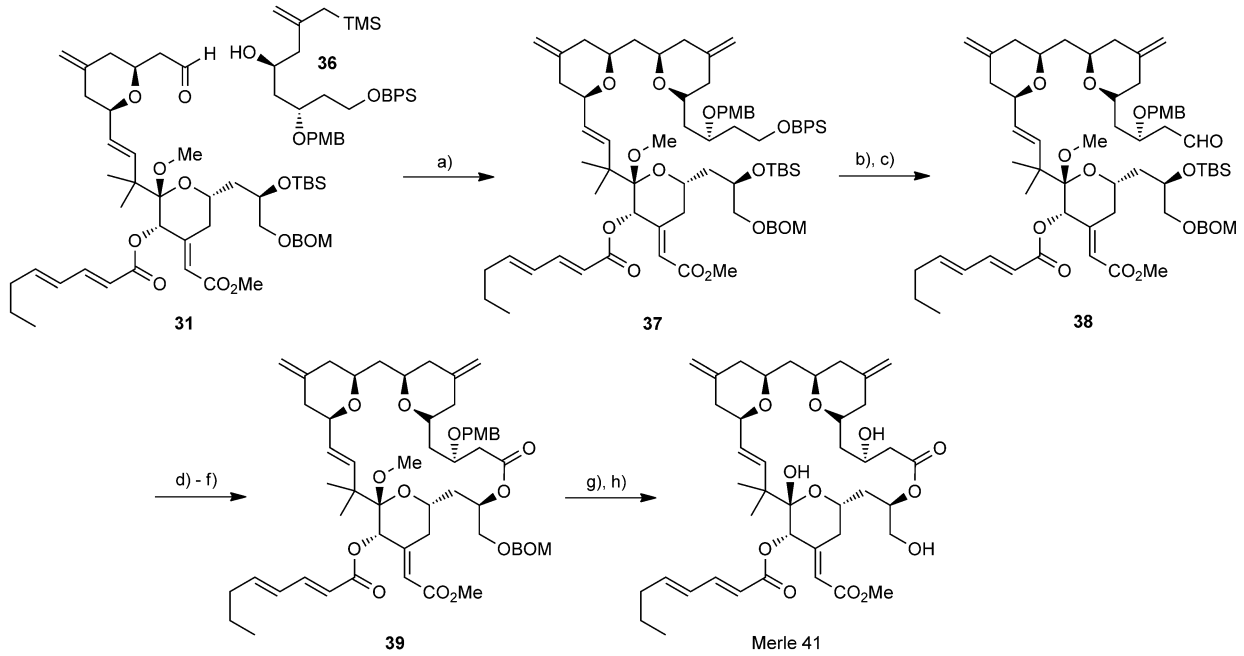

Scheme 9. Completion of the synthesis of Merle 41. a) TMSOTf, Py, Et_2O, −78 °C (90%); b) NH_4F, MeOH, reflux; c) DMP, *t*BuOH, Py, CH_2Cl_2, RT (57% over 2 steps); d) $NaClO_2$, $NaHPO_4$, H_2O, isoamylene, *t*BuOH, MeCN, 0 °C; e) HF·Py (20 *w*%), THF, RT; f) 2,4,6-Cl_3BzCl, DIPEA, DMAP, $PhCH_3$, 30 °C (95% over 3 steps); g) DDQ, pH 6 buffer, CH_2Cl_2, 0 °C; h) $LiBF_4$, H_2O, MeCN, reflux (69% over 2 steps).

in support of the lack of a role for the C26 methyl group in biological activity, it should be noted that the relative dose–response curves for downregulation of the PKC isoforms by Merle 41 do not parallel its in vitro binding potencies, as we described above. Likewise, the marked differences between it and bryostatin 1 in downregulation of the PKC isoforms are not reflected in appreciable differences in their selectivity for in vitro binding. Although the basis for these differences remains unresolved, downregulation represents the interplay of numerous factors, both reflecting the initial ligand–PKC interaction and feedback from downstream consequences, as well as multiple pathways. The profound differences in biological response between bryostatin 1 and Merle 23, as previously reported, illustrated that binding alone was only one element, and we and others have speculated that the different surfaces provided by Merle 23/Merle 41 versus bryostatin 1 might be an important contributor.[23c]

Comparison of the patterns of downregulation at 100 nM levels of the various ligands emphasizes a very important concept (Figure 3). Whereas "PMA-like" or "bryostatin-like" may afford a convenient summary of the pattern of behavior in a system like the U937 cells, detailed characterization shows that different ligands have different patterns of interaction with various PKC isoforms or other C1 domain-containing targets like PKD1. The patterns of downregulation of PKC isoforms by Merle 41 or Merle 23 were unique and distinct from those of either PMA or bryostatin 1. A powerful prediction, therefore, is that such derivatives should have a unique pattern of biology, as we indeed observed in our detailed characterization of the action of Merle 23 in LNCaP cells.[25]

We previously described that PMA initially induced translocation of PKCδ to the plasma membrane of LNCaP cells, with subsequent localization to internal membranes, whereas bryostatin 1 caused less initial plasma membrane translocation, with more staining of nuclear and internal membranes.[38] These differences were likewise found in the current experiments (Figure 4). As previously reported,[25] Merle 23 behaved more like bryostatin 1 than like PMA (Figure 4). Merle 41 behaved similarly to Merle 23 (Figure 4).

PKCε in LNCaP cells was translocated to the plasma membrane in response to PMA and more weakly in response to bryostatin 1 (Figure 5), as had been reported previously.[23b] Merle 23 and Merle 41 resembled one another in their behavior, which was intermediate between that of PMA and bryostatin 1 (Figure 5). Because of the extent of variability of response among cells, it should be noted that the comparisons of translocation for PKCδ and PKCε would not be able to define minor differences in behavior.

As a powerful approach to detect more subtle differences in the responses to Merle 41 and Merle 23, we examined the time and dose dependence of the induction of gene expression by Merle 41 and Merle 23, and we further compared those responses to those induced by PMA and bryostatin 1. Responses were characterized in both LNCaP cells (Figure 6) and U937 cells (Figure 7), two systems that we have studied extensively for their responses to bryostatin derivatives. The genes we examined had been previously observed to illustrate different patterns of response to PMA and bryostatin 1. As we had described before,[39] bryostatin 1 and Merle 23 caused responses in LNCaP cells very similar to those caused by PMA at 2 h (Figure 6A). By 6 h, the response to bryostatin 1 had decreased to variable extents for different genes relative to the PMA response, and the response to Merle 23 began to separate from that of PMA (Figure 6B). By 24 h, the response to Merle 23 had

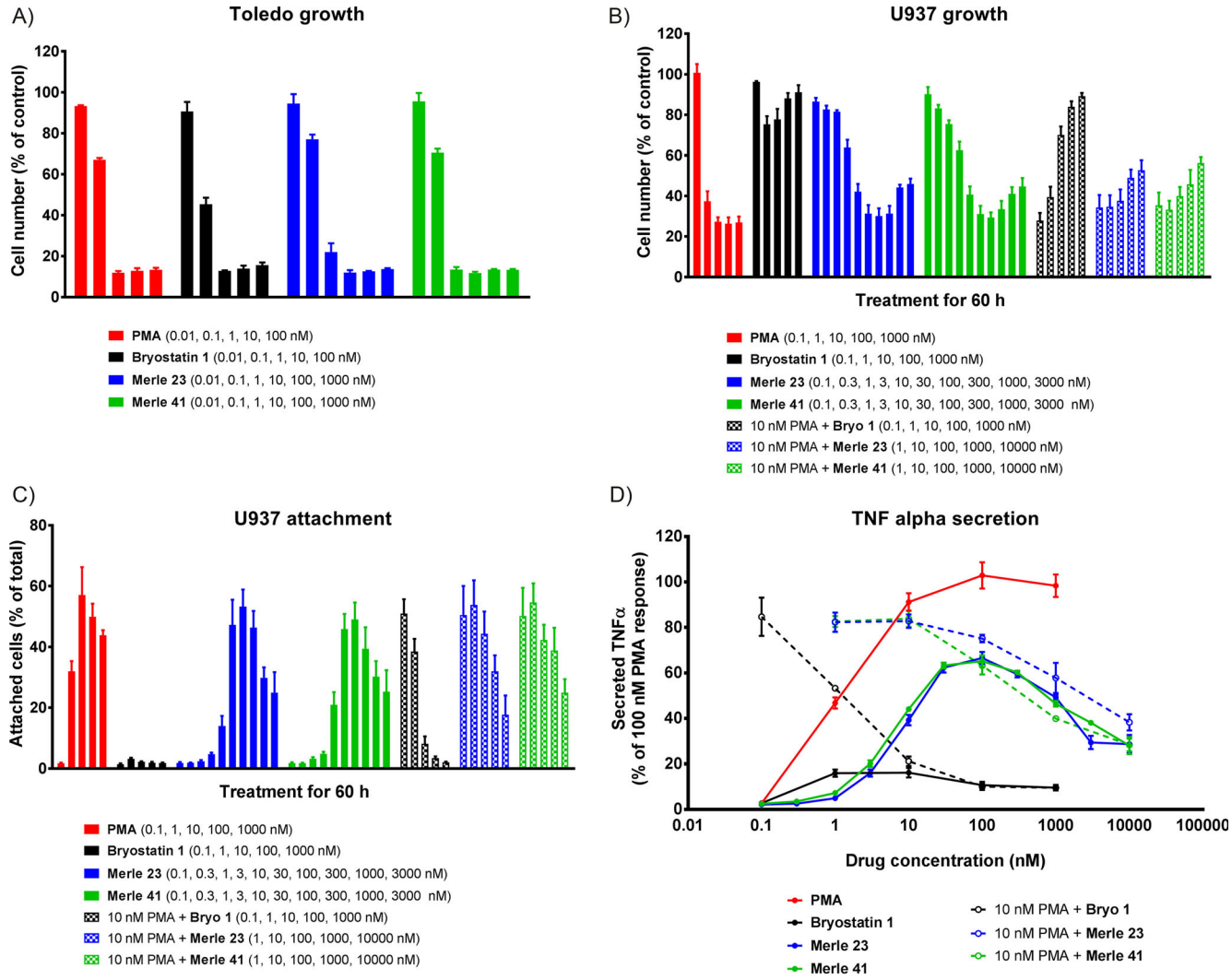

Figure 1. Comparison of the biological effects of Merle 23 and Merle 41. A) Dose–response curves for inhibition of growth of Toledo cells after 72 h of treatment. B) Inhibition of growth of U937 cells after 60 h of treatment. C) Induction of attachment of U937 cells after 60 h of treatment. D) Secretion of TNFα from U937 cells after 60 h of treatment. All points represent the mean ± SEM of triplicate experiments. Methods were as previously described.[23b, 39]

further separated and more approached that of bryostatin 1 (Figure 6C). In each case, the response to Merle 41 was almost identical to that of Merle 23. A similar pattern was observed in the U937 cells, except that the response to bryostatin 1 diverged at later times for some genes, and the response to Merle 23 remained closer to the PMA response (Figure 7). In each case, the response to Merle 41 remained very similar to that of Merle 23.

The above summaries reflect behavior at 100 nM concentrations of each ligand. The complete dose–response curves provide further insight. For example, at 2 h in the U937 cells, the response of TNFAIP3 was greater for bryostatin 1 than it was for PMA or for Merle 23/41 (Figure 7A). The complete dose–response curves revealed that bryostatin 1 was not actually more effective at induction of TNFAIP3 gene expression (Figure 8); rather, the dose–response curves for PMA and Merle 23/41 were markedly biphasic, although that for bryostatin 1 was less so. Equal levels of TNFAIP3 were induced at optimal levels of each ligand, but a 1 nM concentration of PMA and bryostatin 1 gave maximal induction, whereas maximal induction by Merle 23/41 occurred at 10 nM. Because of the biphasic dose–response curves, response to bryostatin 1 at 10 nM was somewhat lower, and response to PMA was lower still. Because the dose–response to bryostatin 1 was substantially less biphasic than that of PMA or Merle 23/41, at 100 nM, the response to bryostatin 1 was greater than that of PMA or Merle 23/41. Despite such complexities, Merle 41 behaved similarly to Merle 23 under virtually all assay conditions. Of the 15 genes examined in LNCaP cells and the 12 genes examined in U937 cells, a modest, statistically significant difference in the responses to Merle 23 and Merle 41 was observed in only one case, for induction of TNFα expression in U937 cells (Figure S1 in the Supporting Information).

Conclusion

Our extensive analysis failed to reveal any substantial influence of the C26 methyl group on the pattern of biological response

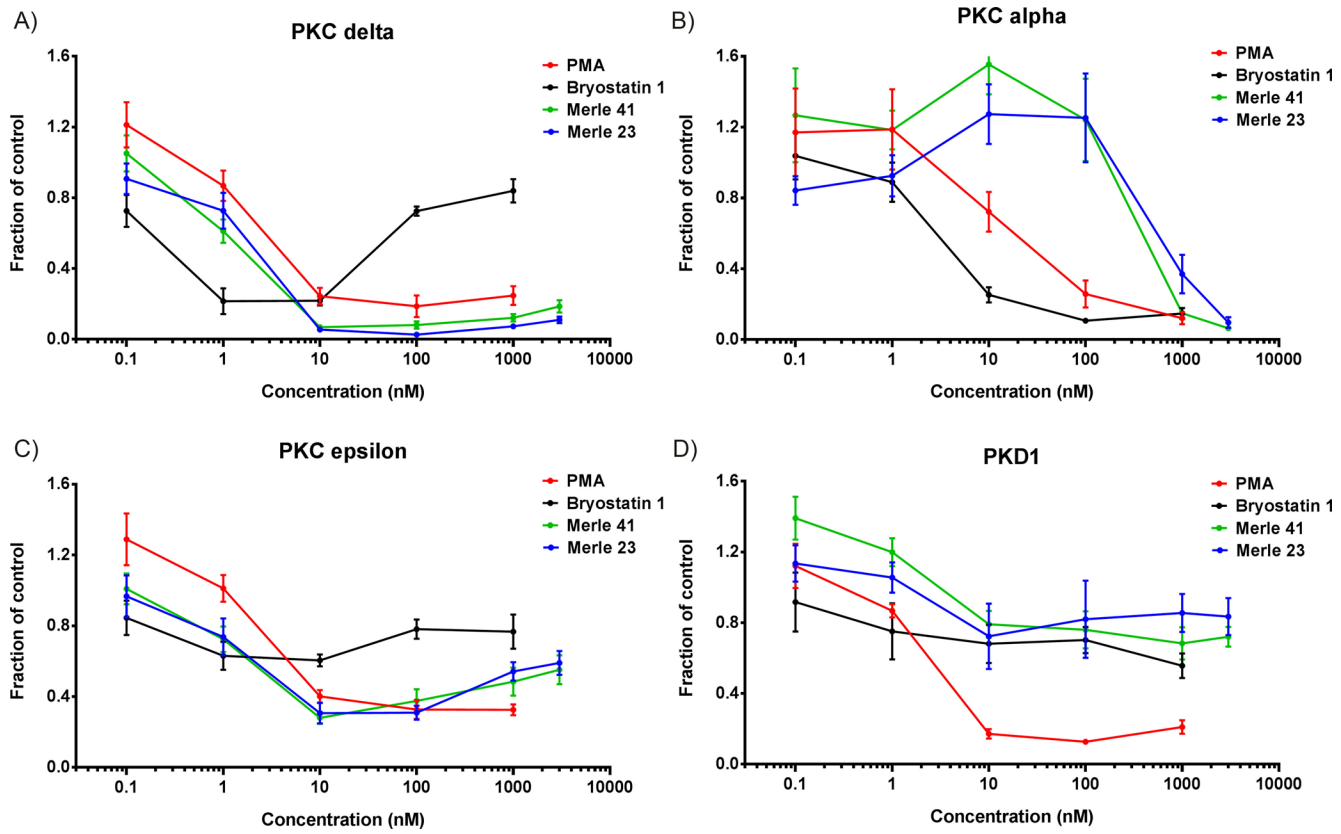

Figure 2. Dose–response curves for downregulation of PKC isoforms and PKD1 in LNCaP cells. LNCaP cells were treated as indicated for 24 h. All points represent the mean ± SEM of quadruplicate experiments. Methods are described in the Supporting Information.

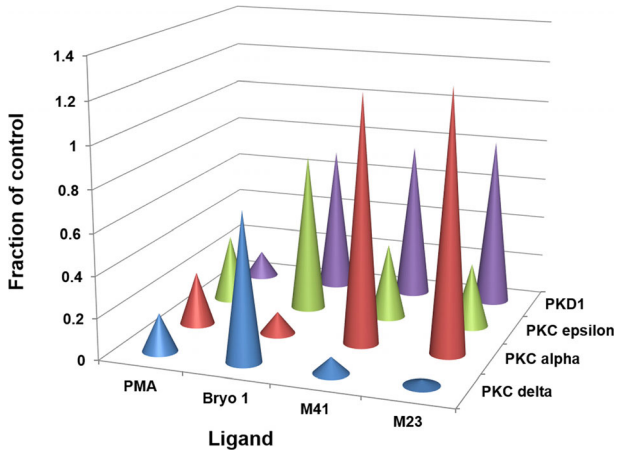

Figure 3. Comparison of the effects of compounds on the levels of PKC isoforms and of PKD1 in LNCaP cells. Levels following treatment for 24 h with the indicated compounds (100 nM) are expressed relative to those for the vehicle control (DMSO; data from Figure 6).

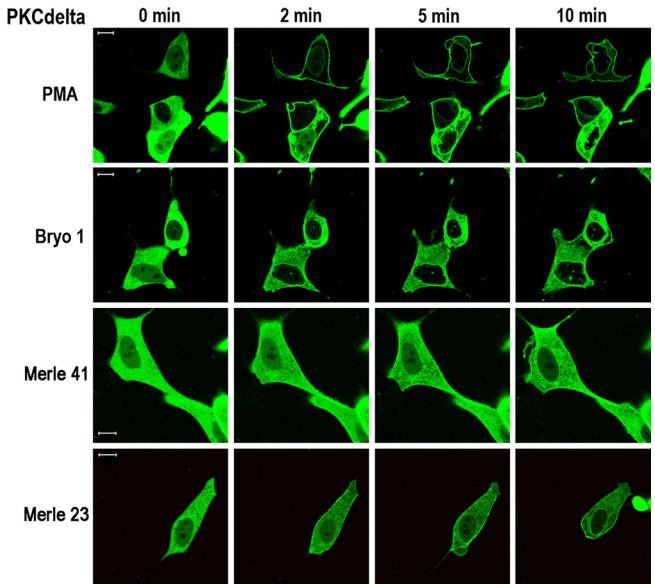

Figure 4. Comparison of the effects of compounds on translocation of mouse GFP-PKCδ. LNCaP cells were imaged at the indicated times after treatment with 1000 nM concentrations of the compounds. Results are representative of five experiments for PMA and bryostatin 1, 12 experiments for Merle 23, and ten experiments for Merle 41. Scale bars: 10 μm. Methods were as previously described.[23b]

of this pair of bryostatin derivatives, Merle 23 and Merle 41. Until shown otherwise, it therefore seems appropriate to assume that differences in bryostatin structure–function relationships reflect structural differences, exclusive of the presence or absence of a C26 methyl group.

As we learn more about bryostatin structure–function relationships, the importance of detailed functional characterization has become ever clearer. PKC binding potency represents an initial determinant of potential activity and is predominantly

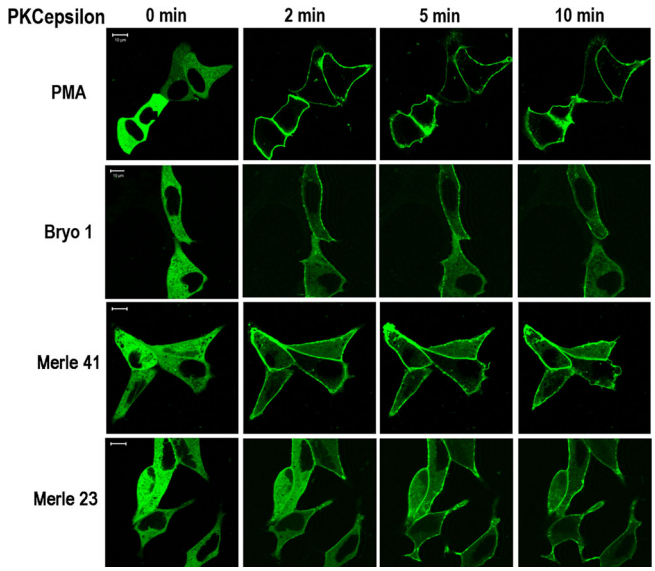

Figure 5. Comparison of the effects of compounds on translocation of human YFP-PKCε. LNCaP cells were imaged at the indicated times after treatment with 1000 nM concentrations of the compounds. Results are representative of 4 experiments for PMA, bryostatin 1, and Merle 23, and six experiments for Merle 41. Scale bars: 10 μm. Methods were as previously described.[23b]

conferred by pharmacophoric elements in the lower half of the molecule.[16] In contrast, the failure of bryostatin 1 to induce PMA-like responses, despite PKC activation, is largely conferred by the top (A, B rings) portion of the molecule,[20,40] provided some domain capable of high affinity PKC binding is present. Bryostatin-like activity is not an all-or-none phenomenon, however. A series of bryostatin derivatives with progressive modifications in the patterns of substitution in the A and/or B ring portion showed variable extents to which they resembled PMA versus bryostatin 1 in their activity in a U937 cell system.[39] The extents of bryostatin-like activity correlated with the extent to which they could induce a more bryostatin-like pattern of transient gene expression. Comparison of the behavior of Merle 23 in U937 cells with its activity in LNCaP cells further emphasized that the cellular pattern of response depended not only on the ligand but also on the cell system.[25] Thus, in LNCaP cells, Merle 23 was like bryostatin 1, not like PMA, in its inability to inhibit cell proliferation. A plausible rationale is that biological responses in different cells show different dependence on the levels of expression of different PKC isoforms and on the variable sensitivities of these isoforms to the compounds. The biological outcome depends on the extent of downregulation of the various isoforms, as well as on their cellular localization.[25,39,41]

An important implication for therapeutic development is that different ligands that cause different patterns of PKC isoform downregulation and localization should have different impacts, depending on the specific cell type and the specific set of responses of importance for that cell. As illustrated here, Merle 23/41 have their own patterns of PKC regulation. These compounds could thus be of particular utility for the appropriate targets. By extension, the current efforts in bryostatin structural modification might yield important drug leads beyond the initial goal of structurally simplified, synthetically accessible bryostatin 1 mimetics.

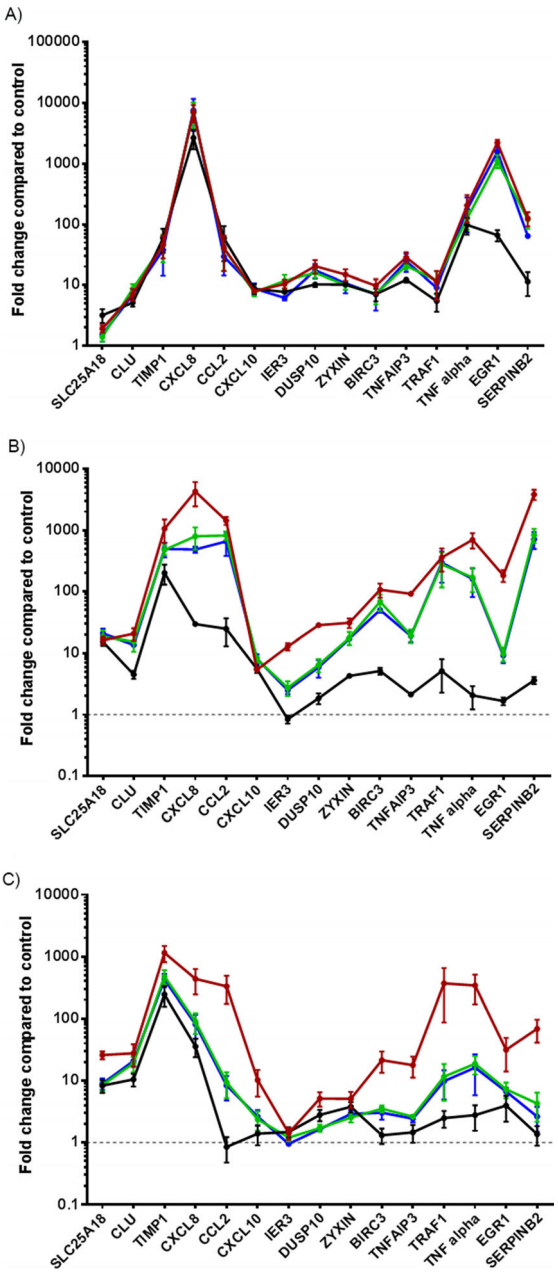

Figure 6. Induction of gene expression in LNCaP cells as a function of time following treatment with 100 nM concentrations of PMA (●), bryostatin 1 (●), Merle 23 (●), and Merle 41 (●). Levels of mRNA expression of the indicated genes were measured by qPCR as described previously[39] after treatment for A) 2 h, B) 6 h, and C) 24 h. Values are expressed relative to those for the vehicle control (DMSO) and represent the mean ± SEM of triplicate experiments.

Acknowledgements

This research was supported in part by the intramural research program of the National Institutes of Health (NIH), Center for

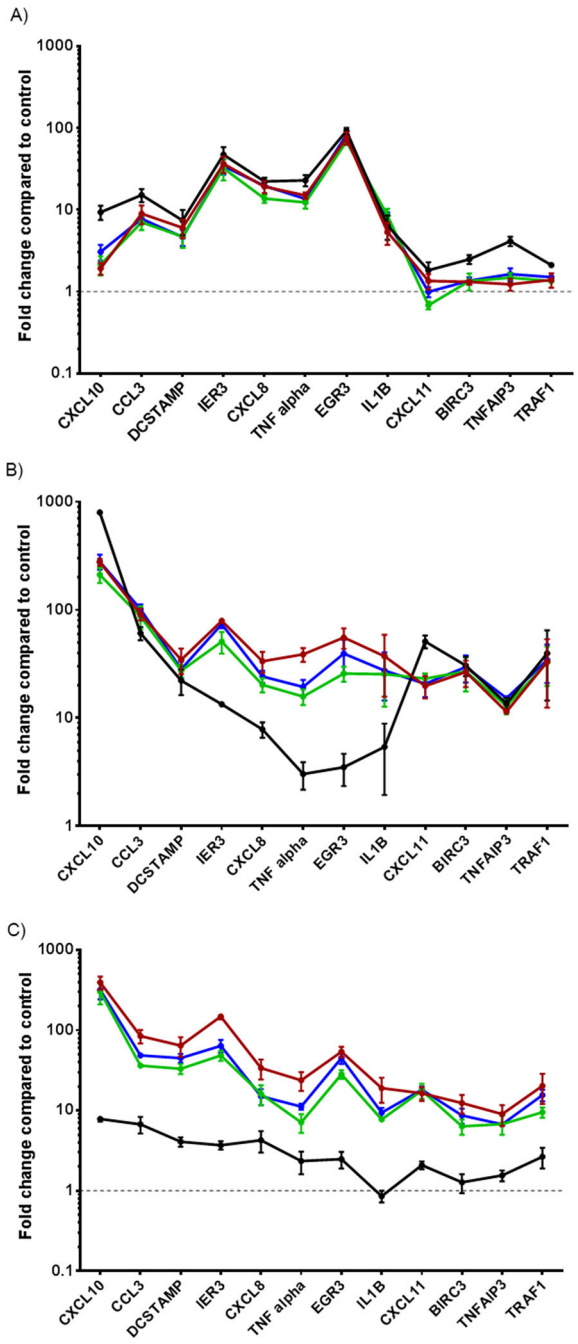

Figure 7. Induction of gene expression in U937 cells as a function of time following treatment with 100 nM concentrations of PMA (●), bryostatin 1 (●), Merle 23 (●), and Merle 41 (●). Levels of mRNA expression of the indicated genes were measured by qPCR as described previously[39] after treatment for A) 2 h, B) 6 h, and C) 24 h. Values are expressed relative to those for the vehicle control (DMSO) and represent the mean ± SEM of triplicate experiments.

Cancer Research, National Cancer Institute (Project Z1A BC 005270) and by an extramural NIH grant (R01 GM 028961 to G.E.K.).

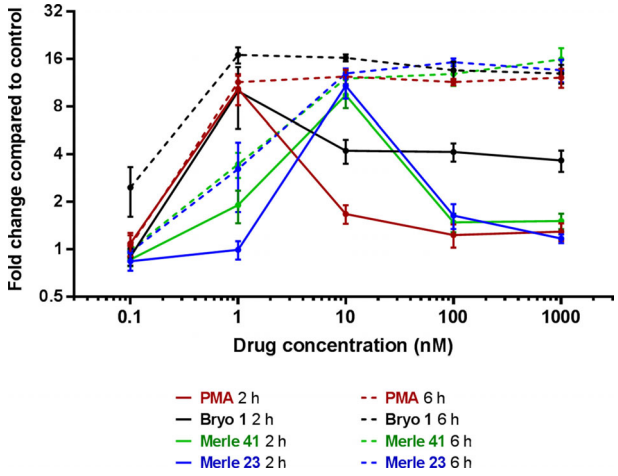

Figure 8. Dose–response for induction of gene expression of TNFAIP3 in U937 cells after treatment for 2 or 6 h. Values are expressed relative to those for the vehicle control (DMSO) and represent the mean ± SEM of triplicate experiments.

Conflict of Interest

The authors declare no conflict of interest.

Keywords: drug design · natural products · protein kinase C · signal transduction · structure–activity relationships

[1] G. R. Pettit, C. L. Herald, D. L. Doubek, D. L. Herald, *J. Am. Chem. Soc.* **1982**, *104*, 6846 – 6848.
[2] a) B. F. Ruan, H. L. Zhu, *Curr. Med. Chem.* **2012**, *19*, 2652 – 2664; b) C. M. Gould, A. C. Newton, *Curr. Drug Targets* **2008**, *9*, 614 – 625.
[3] E. M. Griner, M. G. Kazanietz, *Nat. Rev. Cancer* **2007**, *7*, 281 – 294.
[4] H. Hennings, P. M. Blumberg, G. R. Pettit, C. L. Herald, R. Shores, S. H. Yuspa, *Carcinogenesis* **1987**, *8*, 1343 – 1346.
[5] M. K. Sun, D. L. Alkon, *Adv. Pharmacol.* **2012**, *64*, 273 – 302.
[6] L. N. McKernan, D. Momjian, J. Kulkosky, *Adv. Virol.* **2012**, *2012*, 805347.
[7] For reviews of the bryostatins, see: a) K. J. Hale, M. G. Hummersone, S. Manaviazar, M. Frigerio, *Nat. Prod. Rep.* **2002**, *19*, 413 – 453; b) K. J. Hale, S. Manaviazar, *Chem. Asian J.* **2010**, *5*, 704 – 754; c) B. Halford, *Chem. Eng. News* **2011**, *89*, 10 – 17.
[8] M. Kageyama, T. Tamura, M. H. Nantz, J. C. Roberts, P. Somfai, D. C. Whritenour, S. Masamune, *J. Am. Chem. Soc.* **1990**, *112*, 7407 – 7408.
[9] D. A. Evans, P. H. Carter, E. M. Carreira, J. A. Prunet, A. B. Charette, M. Lautens, *Angew. Chem. Int. Ed.* **1998**, *37*, 2354 – 2359; *Angew. Chem.* **1998**, *110*, 2526 – 2530.
[10] K. Ohmori, Y. Ogawa, T. Obitsu, Y. Ishikawa, S. Nishiyama, S. Yamamura, *Angew. Chem. Int. Ed.* **2000**, *39*, 2290 – 2294; *Angew. Chem.* **2000**, *112*, 2376 – 2379.
[11] G. E. Keck, Y. B. Poudel, T. J. Cummins, A. Rudra, J. A. Covel, *J. Am. Chem. Soc.* **2011**, *133*, 744 – 747.
[12] B. M. Trost, G. Dong, *Nature* **2008**, *456*, 485 – 488.
[13] Y. Lu, S. K. Woo, M. J. Krische, *J. Am. Chem. Soc.* **2011**, *133*, 13876 – 13879.
[14] P. A. Wender, A. J. Schrier, *J. Am. Chem. Soc.* **2011**, *133*, 9228 – 92312.
[15] Y. Zhang, Q. Guo, X. Sun, J. Lu, Y. Cao, Q. Pu, Z. Chu, L. Gao, Z. Song, *Angew. Chem. Int. Ed.* **2018**, *57*, 942 – 946; *Angew. Chem.* **2018**, *130*, 954 – 958.
[16] P. A. Wender, J. Debrabander, P. G. Harran, J. M. Jimenez, M. F. T. Koehler, B. Lippa, C. M. Park, M. Shiozaki, *J. Am. Chem. Soc.* **1998**, *120*, 4534 – 4535.

[17] P. A. Wender, J. Baryza, C. Bennett, C. Bi, S. E. Brenner, M. Clarke, J. Horan, C. Kan, E. Lacote, B. Lippa, P. Nell, T. Turner, *J. Am. Chem. Soc.* **2002**, *124*, 13648 – 13649.
[18] G. E. Keck, J. A. Covel, T. Schiff, T. Yu, *Org. Lett.* **2002**, *4*, 1189 – 1192.
[19] a) G. E. Keck, A. P. Truong, *Org. Lett.* **2005**, **7**, 2149 – 2152; b) G. E. Keck, A. P. Truong, *Org. Lett.* **2005**, *7*, 2153 – 2156.
[20] G. E. Keck, M. B. Kraft, A. P. Truong, W. Li, C. C. Sanchez, N. Kedei, N. E. Lewin, P. M. Blumberg, *J. Am. Chem. Soc.* **2008**, *130*, 6660 – 6661.
[21] J. A. Vrana, A. M. Saunders, S. P. Chellappan, S. Grant, *Differentiation* **1998**, *63*, 33 – 42.
[22] P. A. Wender, B. A. DeChristopher, A. J. Schrier, *J. Am. Chem. Soc.* **2008**, *130*, 6658 – 6659.
[23] For selected examples, see: a) M. B. Kraft, Y. B. Poudel, N. Kedei, N. E. Lewin, M. L. Peach, P. M. Blumberg, G. E. Keck, *J. Am. Chem. Soc.* **2014**, *136*, 13202 – 13208; b) N. Kedei, N. E. Lewin, T. Geczy, J. Selezneva, J. Chen, M. A. Herrmann, M. R. Heldman, L. Lim, P. Mannan, S. H. Garfield, Y. B. Poudel, T. J. Cummins, A. Rudra, P. M. Blumberg, G. E. Keck, *ACS Chem. Biol.* **2013**, *8*, 767 – 777; c) G. E. Keck, Y. B. Poudel, A. Rudra, J. C. Stephens, N. Kedei, N. E. Lewin, M. L. Peach, P. M. Blumberg, *Angew. Chem. Int. Ed.* **2010**, *49*, 4580 – 4584; *Angew. Chem.* **2010**, *122*, 4684 – 4688.
[24] A. DeChristopher, A. C. Fan, D. W. Feisher, P. A. Wender, *Oncotarget* **2012**, *3*, 58 – 66.
[25] N. Kedei, A. Telek, A. Czap, E. S. Lubart, G. Czifra, D. Yang, J. Chen, T. Morrison, P. K. Goldsmith, L. Lim, P. Mannan, S. H. Garfield, M. B. Kraft, W. Li, G. E. Keck, P. M. Blumberg, *Biochem. Pharmacol.* **2011**, *81*, 1296 – 1308.
[26] G. E. Keck, K. H. Tarbet, L. S. Geraci, *J. Am. Chem. Soc.* **1993**, *115*, 8467 – 8468.
[27] G. D. Cuny, S. L. Buchwald, *J. Am. Chem. Soc.* **1993**, *115*, 2066 – 2068.
[28] G. E. Keck, E. P. Boden, S. A. Mabury, *J. Org. Chem.* **1985**, *50*, 709 – 710.
[29] D. B. Dess, J. C. Martin, *J. Am. Chem. Soc.* **1991**, *113*, 7277 – 7287.
[30] A. L. Gemal, J. L. Luche, *J. Am. Chem. Soc.* **1981**, *103*, 5454 – 5459.
[31] J. Inanaga, K. Hirata, H. Saeki, T. Katsuki, M. Yamaguchi, *Bull. Chem. Soc. Jpn.* **1979**, *52*, 1989 – 1993.
[32] G. E. Keck, S. Castellino, *J. Am. Chem. Soc.* **1986**, *108*, 3847 – 3849.
[33] B. S. Bal, W. E. Childers, Jr., H. W. Pinnick, *Tetrahedron* **1981**, *37*, 2091 – 2096.
[34] B. H. Lipshutz, D. F. Harvey, *Synth. Commun.* **1982**, *12*, 267 – 277.
[35] G. E. Keck, Y. B. Poudel, A. Rudra, J. C. Stephens, N. Kedei, N. E. Lewin, M. L. Peach, P. M. Blumberg, *Bioorg. Med. Chem. Lett.* **2012**, *22*, 4084 – 4088.
[36] S. L. Stang, A. Lopez-Campistrous, X. Song, N. A. Dower, P. M. Blumberg, P. A. Wender, J. C. Stone, *Exp. Hematol.* **2009**, *37*, 122 – 134.
[37] I. P. Andrews, J. M. Ketcham, P. M. Blumberg, N. Kedei, N. E. Lewin, M. L. Peach, M. J. Krische, *J. Am. Chem. Soc.* **2014**, *136*, 13209 – 13216.
[38] Q. J. Wang, D. Bhattacharyya, S. Garfield, K. Nacro, V. E. Marquez, P. M. Blumberg, *J. Biol. Chem.* **1999**, *274*, 37233 – 37239.
[39] N. Kedei, A. Telek, A. M. Michalowski, M. B. Kraft, W. Li, Y. B. Poudel, A. Rudra, M. E. Petersen, G. E. Keck, P. M. Blumberg, *Biochem. Pharmacol.* **2013**, *85*, 313 – 324.
[40] N. Kedei, M. B. Kraft, G. E. Keck, C. L. Herald, N. Melody, G. R. Pettit, P. M. Blumberg, *J. Nat. Prod.* **2015**, *78*, 896 – 900.
[41] N. Kedei, J. Q. Chen, M. A. Herrmann, A. Telek, P. K. Goldsmith, M. E. Petersen, G. E. Keck, P. M. Blumberg, *J. Med. Chem.* **2014**, *57*, 5356 – 5369.

Manuscript received: December 19, 2017
Accepted manuscript online: March 8, 2018
Version of record online: ■■ ■■, 0000

*X. Zhao, N. Kedei, A. Michalowski, N. E. Lewin, G. E. Keck, P. M. Blumberg**

■■ – ■■

Deletion of the C26 Methyl Substituent from the Bryostatin Analogue Merle 23 Has Negligible Impact on Its Biological Profile and Potency

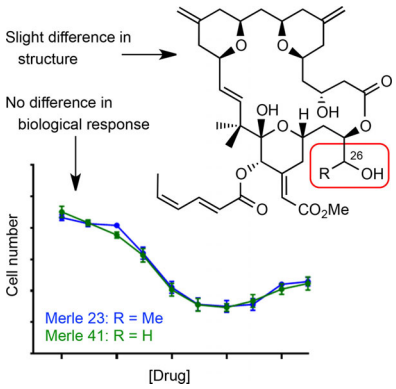

Missing but not missed: Work is underway to understand how bryostatin 1, a potential therapeutic agent for cancer and dementia, confers potency toward protein kinase C and induces unique biological responses. Although the secondary C26 hydroxy group was considered a critical pharmacophoric element, the presence or absence of C26 methyl substitution of bryostatin analogues did not affect their induced biological responses.